Polyhedron 29 (2010) 1497–1507

Contents lists available at ScienceDirect

Polyhedron

journal homepage: www.elsevier.com/locate/poly

Chiral C_1-symmetric 2,2′:6′,2″-terpyridine ligands: Synthesis, characterization, complexation with copper(II), rhodium(III) and ruthenium(II) ions and use of the complexes in catalytic cyclopropanation of styrene

Chi-Tung Yeung [a], Wing-Sze Lee [a], Chui-Shan Tsang [a], Shek-Man Yiu [a], Wing-Tak Wong [b], Wai-Yeung Wong [c], Hoi-Lun Kwong [a,*]

[a] Department of Biology and Chemistry and Open Laboratory of Chirotechnology of the Institute of Molecular Technology for Drugs Discovery and Synthesis, City University of Hong Kong, Tat Chee Avenue, Kowloon, Hong Kong, China
[b] Department of Chemistry, The University of Hong Kong, Pokfulam Road, Hong Kong, China
[c] Department of Chemistry, Hong Kong Baptist University, Waterloo Road, Hong Kong, China

ARTICLE INFO

Article history:
Received 3 September 2009
Accepted 13 January 2010
Available online 20 January 2010

Keywords:
Chiral terpyridine
Copper
Rhodium
Ruthenium
Metal-catalyzed cyclopropanation
Asymmetric catalysis

ABSTRACT

Three new optically pure C_1-terpyridine ligands (**L1**–**3**) were prepared and the copper(II) complexes, of formula [Cu(**L**)Cl_2], the rhodium(III) complexes, of formula [Rh(**L**)Cl_3], and the ruthenium(II) complexes, of formula *cis*- or *trans*-[Ru(**L**)(X)Cl_2] (X = DMSO or CO), were synthesized. Structures of a chiral C_1-ligand, a copper complex, a rhodium complex and a ruthenium DMSO complex were analysed using X-ray crystal structure analysis. The copper, rhodium and ruthenium complexes were shown to be precursors of catalysts for cyclopropanation. Reaction of [Cu(**L**)Cl_2], [Rh(**L**)Cl_3] or *cis*- or *trans*-[Ru(**L**)(X)Cl_2] with AgOTf converted the complex to catalyst, which in the case of *trans*-[Ru(**L**)(CO)Cl_2] gave enantioselectivities of up to 67% ee for the *cis*-isomers of styrene cyclopropanes with *t*-butyl diazoacetate. Comparisons with C_2-analog of copper, rhodium and ruthenium catalysts were made.

1. Introduction

2,2′:6′,2″-Terpyridine (tpy) ligands are of great interest in many research fields [1–4]. One such area is supramolecular chemistry, as tpy can form supermolecular self-assembly through coordination with metal ions [5–8]. Recently, we have been reported the use of chiral C_2-symmetric tpy for supramolecular assembly which can be used in catalysis [9]. The development of new chiral version of tpy should lead to more interesting supermolecular architectural structure and interesting new catalysts. In this study, we report three new C_1-tpy **L1**–**3** and their copper, rhodium and ruthenium complexes, which are of formula [Cu(**L**)Cl_2], [Rh(**L**)Cl_3] and *cis*- or *trans*-[Ru(**L**)(X)Cl_2] (X = DMSO or CO), respectively. The use of some of these complexes in cyclopropanation are demonstrated. To the best of our knowledge, the use of ruthenium terpyridine complexes have not been reported to be efficient catalysts in the cyclopropanation of olefins before [10]. Comparisons between C_1- and analog C_2-symmetric ligands, **L4**–**6**, of similar complexes have been made.

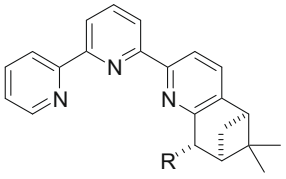

L1: R = H
L2: R = methyl

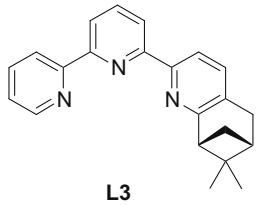

L3

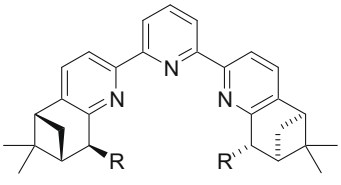

L4: R = H
L5: R = methyl

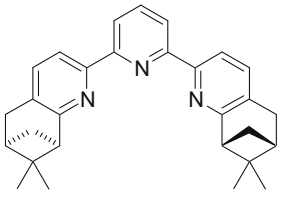

L6

* Corresponding author. Tel.: +852 27777304; fax: +852 27887406.
E-mail address: bhhoik@cityu.edu.hk (H.-L. Kwong).

0277-5387/$ - see front matter © 2010 Elsevier Ltd. All rights reserved.
doi:10.1016/j.poly.2010.01.017

2. Experimental

2.1. General information

All reactions were carried out under a dinitrogen atmosphere using standard Schlenk techniques. Dichloromethane was distilled over calcium hydride. THF was distilled under N_2 over sodium/benzophenone. Ethyl diazoacetate, *t*-butyl diazoacetate and $[RuCl_2(p\text{-cymene})]_2$ of reagent-grade quality were obtained commercially. Ligands **L4–6** were prepared as previously described [11–13]. Chiral α,β-unsaturated ketones (1*R*,5*R*)-6,6-dimethyl-2-methylenebicyclo[3.1.1]heptan-3-one, (1*R*,4*S*,5*R*)-4,6,6-trimethyl-2-methylenebicyclo[3.1.1]heptan-3-one and (1*R*,5*R*)-6,6-dimethyl-3-methylenebicyclo[3.1.1]heptan-2-one were prepared in good overall yields from (−)-β-pinene and (1*R*,2*R*,3*R*,5*S*)-(−)-isopinocamphenol according to literature procedures [13,14]. 2-Acetyl-6-bromopyridine [15], 6-acetyl-2,2′-bipyridine [15] and 6-(1-pyridinioacetyl)-2,2′-bipyridine iodide [16] were prepared as previously described. Infrared spectra in the range 500–4000 cm^{-1} as KBr plates were recorded on a Perkin Elmer Model FT-IR-1600 spectrometer. ^1H and ^{13}C NMR spectra were recorded on a Varian 300 MHz Mercury instrument. Positive ion mass spectra were taken by PE SCIEX API 365 electro-spray mass spectrometer. Elemental analyses were performed on a Vario EL elemental analyzer. Optical rotations were measured by JASCO DIP-370 digital polarimeter. Melting points were measured by electrothermal digital melting point apparatus.

2.2. General procedure for synthesis of terpyridines *L1–3*

The ligands were synthesized by Kröhnke condensation [17]. 6-(1-Pyridinoacetyl)-2,2′-bipyridine iodide (1.5 mmol, 0.58 g), α,β-unsaturated ketone (2 mmol) and ammonium acetate (25.9 mmol, 2 g) were dissolved in glacial acetic acid (2 mL). The mixture was refluxed (120 °C) for 12 h. Reaction was quenched by the addition of saturated $NaHCO_3$ and then extracted with Et_2O (50 mL × 3). Solvent was removed under reduced pressure and brown residue was purified by recrystallization. Products were characterized by IR, ^1H NMR, ^{13}C NMR and MS.

L1. With ketone (1*R*,5*R*)-6,6-dimethyl-2-methylenebicyclo[3.1.1]heptan-3-one, after workup and purification by recrystallization with acetonitrile, the procedure gave 0.31 g (63%) **L1**: mp 153–155 °C; $[\alpha]_D^{25} = -80.7°$ ($c = 0.31$, CH_2Cl_2); ^1H NMR (300 MHz, $CDCl_3$): δ 0.70 (s, 3H), 1.34 (d, $J = 9.9$ Hz, 1H), 1.44 (s, 3H), 2.42–2.46 (m, 1H), 2.71–2.78 (m, 1H), 2.84–2.89 (m, 1H), 3.27–3.30 (m, 2H), 7.32–7.38 (m, 1H), 7.41–7.46 (m, 1H), 7.85–7.99 (m, 2H), 8.31–8.35 (m, 1H), 8.42–8.53 (m, 2H), 8.63–8.66 (m, 1H), 8.71–8.73 (m, 1H); ^{13}C NMR ($CDCl_3$): δ 21.59, 25.70, 31.27, 35.68, 39.31, 39.64, 46.70, 118.32, 120.61, 120.72, 121.08, 126.56, 135.25, 139.17, 142.04, 144.18, 146.39, 146.95, 148.69, 149.15, 150.18, 159.72; ESI-MS (MeOH) *m/z*: 328 $[M+H]^+$.

L2. With ketone (1*R*,4*S*,5*R*)-4,6,6-trimethyl-2-methylenebicyclo[3.1.1]heptan-3-one, after workup and purification by recrystallization with acetonitrile, the procedure gave 0.23 g (44%) **L2**: mp 149–151 °C; $[\alpha]_D^{25} = -58.5°$ ($c = 0.33$, CH_2Cl_2); ^1H NMR (300 MHz, $CDCl_3$): δ 0.69 (s, 3H), 1.35 (d, $J = 9.6$ Hz, 1H), 1.44 (s, 3H), 1.49 (d, $J = 7.2$ Hz, 3H), 2.18–2.21 (m, 1H), 2.56–2.63 (m, 1H), 2.81–2.85 (m, 1H), 3.27–3.29 (m, 1H), 7.30–7.37 (m, 2H), 7.83–7.88 (m, 1H), 7.91–7.96 (m, 1H), 8.29 (d, $J = 7.8$ Hz, 1H), 8.40 (d, $J = 7.5$ Hz, 1H), 8.50 (d, $J = 7.8$ Hz, 1H), 8.63 (d, $J = 7.5$ Hz, 1H), 8.70 (d, $J = 4.2$ Hz, 1H); ^{13}C NMR ($CDCl_3$): δ 18.26, 20.94, 26.37, 28.66, 38.95, 41.50, 46.92, 47.29, 117.86, 120.29, 120.76, 121.17, 123.56, 133.42, 136.75, 137.66, 142.16, 149.07, 153.46, 155.17, 156.19, 156.57, 160.21; ESI-MS (MeOH) *m/z*: 342 $[M+H]^+$.

L3. With ketone (1*R*,5*R*)-6,6-dimethyl-3-methylenebicyclo[3.1.1]heptan-2-one, after workup and purification by recrystallization with acetonitrile, the procedure gave 0.35 g (57%) **L3**: mp 126–128 °C; $[\alpha]_D^{25} = -58.5°$ ($c = 0.33$, CH_2Cl_2); ^1H NMR (300 MHz, $CDCl_3$): δ 0.72 (s, 3H), 1.37 (d, $J = 9.6$ Hz, 1H), 1.46 (s, 3H), 2.35–2.39 (m, 1H), 2.76 (dt, $J = 9.7$, 3.8 Hz, 1H), 3.02 (d, $J = 5.3$ Hz, 2H), 3.15 (t, $J = 5.3$ Hz, 1H), 7.31–7.36 (m, 1H), 7.59 (d, $J = 7.9$ Hz, 1H), 7.86 (td, $J = 7.6$, 1.8 Hz, 1H), 7.93 (t, $J = 7.9$ Hz, 1H), 8.39 (d, $J = 7.6$ Hz, 1H), 8.40 (dd, $J = 7.9$, 0.9 Hz, 1H), 8.45 (dd, $J = 7.9$, 0.9 Hz, 1H), 8.62–8.65 (m, 1H), 8.69–8.71 (m, 1H); ^{13}C NMR ($CDCl_3$): δ 21.31, 26.05, 30.91, 31.31, 39.20, 40.15, 50.45, 118.88, 120.40, 120.95, 121.19, 123.65, 130.71, 135.99, 136.84, 137.78, 149.04, 152.03, 155.15, 155.83, 156.39, 165.80; ESI-MS (MeOH) *m/z*: 328 $[M+H]^+$. Single crystals of **L3** suitable for X-ray diffraction analysis were obtained by slow evaporation of a CH_2Cl_2 solution.

2.3. General procedure for preparation of [Cu(*L*)Cl_2] (*L* = *L13*)

A solution of **L** (0.2 mmol) in CH_2Cl_2 (2.5 mL) was added dropwise to a solution of $CuCl_2{\cdot}2H_2O$ (34 mg, 0.2 mmol) in ethanol (2.5 mL). The reaction mixture was stirred at reflux for 3 h. The solution was then cooled to room temperature and diethyl ether was added until a precipitate was formed. The product was filtered and washed with diethyl ether. The complex was characterized by ESI-MS and elemental analyses.

[Cu(L1)Cl_2]. The above procedure was followed using **L1** to give 82 mg product (89%). *Anal.* Calc. for $C_{22}H_{21}N_3CuCl_2{\cdot}(H_2O)_{0.5}$: C, 56.10; H, 4.67; N, 8.93. Found: C, 56.25; H, 4.67; N, 9.01%; ESI-MS (MeOH): *m/z* 425.3 $[M-Cl]^+$.

[Cu(L2)Cl_2]. The above procedure was followed using **L2** to give 89 mg product (95%). *Anal.* Calc. for $C_{23}H_{23}N_3CuCl_2{\cdot}(H_2O)$: C, 55.92; H, 5.06; N, 8.51. Found: C, 56.09; H, 5.03; N, 8.50%; ESI-MS (MeOH): *m/z* 439.6 $[M-Cl]^+$.

[Cu(L3)Cl_2]. The above procedure was followed using **L3** to give 87 mg product (94%). *Anal.* Calc. for $C_{22}H_{21}N_3CuCl_2{\cdot}(H_2O)_{2.5}$: C, 52.11; H, 5.13; N, 8.30. Found: C, 51.57; H, 5.08; N, 8.48%; ESI-MS (MeOH): *m/z* 425.3 $[M-Cl]^+$.

2.4. General procedure for preparation of [Rh(*L*)Cl_3] (*L* = *L13*)

A mixture of **L** (0.2 mmol) and $RhCl_3{\cdot}3H_2O$ (53 mg, 0.2 mmol) in ethanol (10 mL) was stirred at reflux for 5 h. After cooling to room temperature, the solvent was removed under reduced pressure. The product was recrystallized from CH_2Cl_2/Et_2O to give yellow solid, which was filtered and washed with diethyl ether. The complex was characterized by ^1H NMR, ESI-MS and elemental analyses.

[Rh(L1)Cl_3]. The above procedure was followed using **L1** to give 98 mg product (91%). ^1H NMR ($CDCl_3$): δ 0.71 (s, 3H), 1.38 (d, $J = 9.7$ Hz, 1H), 1.43 (s, 3H), 2.55–2.62 (m, 1H), 2.69–2.76 (m, 1H), 2.91 (t, $J = 5.86$ Hz, 1H), 4.08–4.24 (m, 2H), 7.55 (d, $J = 7.6$ Hz, 1H), 7.67 (t, $J = 6.7$ Hz, 1H), 7.90 (t, $J = 7.9$ Hz, 1H), 8.02 (t, $J = 7.6$ Hz, 1H), 8.12–8.18 (m, 4H), 9.91 (d, $J = 5.6$ Hz, 1H); $C_{22}H_{21}N_3RhCl_3{\cdot}(H_2O)_2$: C, 46.10; H, 4.37; N, 7.34. Found: C, 45.85; H, 4.35; N, 7.32%; ESI-MS (MeOH): *m/z* 500.4 $[M-Cl]^+$.

[Rh(L2)Cl_3]. The above procedure was followed using **L2** to give 90 mg product (82%). ^1H NMR ($CDCl_3$): δ 0.77 (s, 3H), 1.45 (s, 3H), 1.57 (d, $J = 9.7$ Hz, 1H), 1.73 (d, $J = 6.7$ Hz, 3H), 2.31–2.35 (m, 1H), 2.56–2.63 (m, 1H), 2.89 (t, $J = 5.86$ Hz, 1H), 4.89–4.93 (m, 1H), 7.52 (d, $J = 7.6$ Hz, 1H), 7.59 (t, $J = 13.2$ Hz, 1H), 7.90–7.98 (m, 2H), 8.14–8.20 (m, 4H), 9.90 (d, $J = 5.5$ Hz, 1H); $C_{23}H_{23}N_3RhCl_3?(CH_3CH_2OH)_{0.5}$: C, 50.22; H, 4.53; N, 7.32. Found: C, 50.52; H, 4.54; N, 7.37%; ESI-MS (MeOH): *m/z* 414.3 $[M-Cl]^+$.

[Rh(L3)Cl_3]. The above procedure was followed using **L3** to give 92 mg product (86%). ^1H NMR ($CDCl_3$): δ 0.87 (s, 3H), 1.29 (d, $J = 10.4$ Hz, 1H), 1.61 (s, 3H), 2.37–2.42 (m, 1H), 2.86–2.95 (m, 1H), 3.12–3.15 (m, 2H), 5.60 (t, $J = 5.5$ Hz, 1H), 7.68–7.76 (m, 2H),

7.92 (d, J = 8.0 Hz, 1H), 8.03–8.21 (m, 5H), 9.93 (d, J = 5.5 Hz, 1H); $C_{22}H_{21}N_3RhCl_3\cdot(H_2O)_2$: C, 46.10; H, 4.37; N, 7.34. Found: C, 46.10; H, 4.44; N, 7.46%; ESI-MS (MeOH): m/z 500.3 $[M-Cl]^+$.

2.5. General procedure for preparation of [Ru(**L**)Cl$_2$] (**L = L1, L2 and L5**)

Ligand **L** (0.20 mmol) and $[RuCl_2(p\text{-cymene})]_2$ (61 mg, 0.1 mmol) were refluxed in degassed ethanol (10 mL) for 2 days. The resulting deep purple or brown solution was cooled to room temperature and filtered under nitrogen to remove any of undissolved black solid. The solvent was then removed under reduced pressure. The residue was washed with dried Et_2O (10 mL × 3), filtered and dried under vacuum to afford deep purple or deep reddish brown solids. For [Ru(**L1**)Cl$_2$], the yield was 98%. For [Ru(**L2**)Cl$_2$], the yield was 96%. For [Ru(**L5**)Cl$_2$], degassed *n*-butanol was used and the reaction was refluxed for 4 days. The yield was 32%.

2.6. Procedure for preparation of cis-[Ru(**L1**)(DMSO)Cl$_2$]

[Ru(**L1**)Cl$_2$] was dissolved in degassed CH_2Cl_2 (5 mL) at room temperature. Then DMSO (0.2 mmol, 7.1 μL) was added and the solution was stirred for 2 h. Solvent was reduced to ca. 1 mL under vacuum and then Et_2O (20 mL) was added. The deep brown solid was filtered and washed with Et_2O (10 mL × 3). Recrystallization from acetonitrile yielded crystal of the desired product of 102 mg (88%). IR (KBr) ν = 1086.2 cm^{-1} s (SO); ^{1}H NMR ($CDCl_3$, two isomers were observed in a ratio of 1:1): δ 0.71 (s, 3H), 0.76 (s, 3H), 1.21 (d, J = 10.6 Hz, 1H), 1.38 (d, J = 10.0 Hz, 1H), 1.42 (s, 3H), 1.45 (s, 3H), 2.55–2.59 (m, 2H), 2.68 (s, 3H), 2.71 (s, 3H), 2.75–2.80 (m, 2H), 2.87–2.91 (m, 2H), 2.93 (s, 3H), 2.99 (s, 3H), 3.62–4.03 (m, 4H), 7.46 (dd, J = 7.9, 1.5 Hz, 2H), 7.58–7.62 (m, 2H), 7.78–7.83 (m, 4H), 7.89–7.97 (m, 6H), 8.06 (d, J = 7.6 Hz, 2H), 9.62 (d, 5.9 Hz, 2H); *Anal.* Calc. for $C_{24}H_{27}N_3SORuCl_2\cdot(MeCN)_{0.25}(H_2O)$: C, 48.57; H, 4.92; N, 7.52. Found: C, 48.35; H, 4.81; N, 7.53%; ESI-MS (MeOH): m/z 542.4 $[M-Cl]^+$.

2.7. General procedure for preparation of trans-[Ru(**L**)(CO)Cl$_2$] (**L = L2 and L5**)

[Ru(**L**)Cl$_2$] (0.1 mmol) was dissolved in degassed CH_2Cl_2 (5 mL) at room temperature. Then carbon monoxide was bubbled into the reaction mixture for 15 min and the color of the mixture changed from purple to deep brown. Solvent was then reduced to ca. 1 mL under vacuum and Et_2O (20 mL) was added. The deep brown solid was filtered and washed with Et_2O (10 mL × 3) to give the desired product. The products were characterized by IR, ^{1}H NMR, ^{13}C NMR, elemental analyses and ESI-MS.

[Ru(L2)(CO)Cl$_2$]. The above procedure was followed using **L2** to give 48 mg product (89%). IR (KBr) ν = 1946.5 cm^{-1} versus (CO); ^{1}H NMR ($CDCl_3$): δ 0.70 (s, 3H), 1.46 (s, 3H), 1.49 (d, J = 10.3 Hz, 1H), 1.86 (d, J = 6.7 Hz, 3H), 2.35–2.40 (m, 1H), 2.57–2.64 (m, 1H), 2.82 (t, J = 5.6 Hz, 1H), 3.94–4.02 (m, 1H), 7.33 (d, J = 7.9 Hz, 1H), 7.35 (t, J = 6.6 Hz, 1H), 7.75 (t, J = 7.9 Hz, 1H), 7.83 (d, J = 7.6 Hz, 1H), 8.00–8.13 (m, 4H), 9.09 (d, J = 4.7 Hz, 1H); ^{13}C NMR ($CDCl_3$): δ 20.05, 21.02, 25.78, 27.86, 41.73, 42.58, 47.78, 48.22, 120.74, 121.12, 121.24, 123.42, 126.83, 134.55, 136.73, 138.55, 146.97, 154.62, 155.33, 156.99, 157.12, 158.17, 168.76, 206.00 (CO); *Anal.* Calc. for $C_{24}H_{23}N_3ORuCl_2\cdot(MeOH)\cdot(H_2O)$: C, 50.80; H, 4.91; N, 7.11. Found: C, 51.20; H, 5.05; N, 7.30%; ESI-MS (MeOH): m/z 508.1 $[M-Cl]^+$, 392.1 $[M-2Cl]^{2+}$.

[Ru(L5)(CO)Cl$_2$]. The above procedure was followed using **L5** and 1-butanol (10 mL) as solvent. The reaction was refluxed for 4 days to give 53 mg product (82%). IR (KBr) ν = 1947.6 cm^{-1} versus (CO); ^{1}H NMR ($CDCl_3$): δ 0.76 (s, 6H), 1.41 (d, J = 11.1 Hz, 2H), 1.45 (s, 6H), 1.80 (d, J = 7.0 Hz, 6H), 2.38–2.39 (m, 2H), 2.54–2.57 (m, 2H), 2.78–2.79 (m, 2H), 4.26–4.29 (m, 2H), 7.28 (s, 2H), 7.88–8.14 (m, 5H); ^{13}C NMR ($CDCl_3$): δ 20.53, 20.89, 25.62, 27.69, 41.26, 41.83, 47.74, 48.42, 120.77, 121.03, 134.68, 138.64, 146.49, 156.15, 156.35, 170.61, 209.60 (CO); *Anal.* Calc. for $C_{32}H_{35}N_3ORuCl_2?(CH_2Cl_2)$: C, 53.95; H, 5.04; N, 5.72. Found: C, 53.67; H, 4.94; N, 5.65%; ESI-MS (MeOH) m/z: 616.7 $[M-Cl]^+$.

2.8. X-ray structure analysis

Crystallographic data for **L3**, [Cu(**L3**)Cl$_2$], [Rh(**L1**)Cl$_3$] and *cis*-[Ru(**L1**)(DMSO)Cl$_2$] are tabulated in Table 1. For the data collections, intensity data for **L3** was collected on a Bruker SMART CCD area detector using graphite monochromator with Mo Kα radiation (λ = 0.7107 Å), while the data for [Rh(**L1**)Cl$_3$] was collected on a Bruker SMART 1000 CCD area detector. The intensity data for [Cu(**L3**)Cl$_2$] and *cis*-[Ru(**L1**)(DMSO)Cl$_2$] were collected on a Oxford Diffraction Gemini S Ultra X-ray single crystal diffractometer with Mo Kα radiation (λ = 0.7107 Å) and processed using CrysAlis. For the structure solutions, all the structures were solved with SHELXS-97. For the structures refinements, **L3**, [Cu(**L3**)Cl$_2$] and [Ru(**L1**)(DMSO)Cl$_2$] were refined on F^2 with SHELXL-97 (Sheldrick 1997). The structure of [Rh(**L1**)Cl$_3$] was refined on F^2 with SHELXL (Sheldrick 2008). Crystallographic data for the structures have been deposited with the Cambridge Crystallographic Data Center as Supplementary Publication Numbers CCDC 703308, 736281–736283.

2.9. Procedure for copper-catalyzed cyclopropanation reactions

To a mixture of [Cu(**L**)Cl$_2$] (0.02 mmol) and AgOTf (0.04 mmol) in a two-necked pear-shaped flask was added CH_2Cl_2 (2 mL) under nitrogen. The reaction mixture was stirred in the dark at room temperature for 30 min. After filtration, styrene (4 mmol) and ethyl diazoacetate (0.2 mmol) were added and the mixture was stirred at room temperature for 30 min. A solution of ethyl diazoacetate (1 mmol) in CH_2Cl_2 (0.5 mL) was slowly added over 4 h. After the addition of ethyl diazoacetate, the mixture was allowed to stir for 16 h at room temperature. The crude product was purified by column chromatography (petroleum ether/EtOAc). All of the cyclopropanes obtained are known compounds and were characterized by ^{1}H, ^{13}C NMR, IR and GC–MS. Enantiomeric excesses of the cyclopropanes were determined by HPLC with a Daicel Chiralcel OJ column. Absolute configurations were determined by comparing the order of elution of samples with a known configuration. Diastereoselectivities were measured by GC-FID with Ultra 2 crosslinked 5% PhMesilcone (25 m × 0.2 mm × 0.33 μm film thickness).

2.10. Procedure for rhodium-catalyzed cyclopropanation reactions

To a mixture of [Rh(**L**)Cl$_3$] (0.02 mmol) and AgOTf (0.08 mmol) in a two-necked pear-shaped flask was added THF (1.5 mL) under nitrogen. The reaction mixture was stirred in the dark at room temperature for 30 min. After filtration, styrene (5 mmol) was added to the mixture. A solution of ethyl diazoacetate (1 mmol) in THF (0.5 mL) was slowly added over 4 h. After the addition of ethyl diazoacetate, the mixture was allowed to stir for 16 h at room temperature. The mixture was worked-up as described above.

2.11. Procedure for ruthenium-catalyzed cyclopropanation reactions and competition experiments

To a mixture of [Ru(**L**)(CO)Cl$_2$] (0.02 mmol) and AgOTf (0.04 mmol) in a two-necked pear-shaped flask was added CH_2Cl_2 (1.25 mL) under nitrogen. The reaction mixture was stirred in the dark at room temperature for 30 min. After filtration, styrene

Table 1
General crystallographic data for **L3**, [Cu(**L3**)Cl_2], [Rh(**L1**)Cl_3] and *cis*-[Ru(**L1**)(DMSO)Cl_2].

	L3	[Cu(**L3**)Cl_2]	[Rh(**L1**)Cl_3]	*cis*-[Ru(**L1**)(DMSO)Cl_2]
Formula	$C_{22}H_{21}N_3$	$C_{24}H_{23}Cl_8CuN_3$	$C_{69}H_{79}Cl_9N_9Rh_3O_5$	$C_{24}H_{27}Cl_2ORuSN_3$
M	327.42	700.59	1742.19	577.52
Crystal size/mm^3	0.32 × 0.26 × 0.24	0.4 × 0.3 × 0.2	0.42 × 0.10 × 0.06	0.4 × 0.3 × 0.1
Temperature	293(2)	193(2)	301(2)	173(2)
Crystal system	orthorhombic	triclinic	trigonal	orthorhombic
Space group	$P2_12_12_1$	$P\bar{1}$	$R\bar{3}$	$P2_12_12_1$
a (Å)	6.6714(4)	9.6360(4)	24.930(2)	12.2925(2)
b (Å)	13.8836(8)	10.6966(4)	24.930(2)	16.3747(3)
c (Å)	19.335(1)	14.7297(6)	10.389(1)	23.2165(5)
α (°)	90.00	73.475(4)	90.00	90.00
β (°)	90.00	88.096(3)	90.00	90.00
γ (°)	90.00	79.433(3)	120.00	90.00
V (Å^3)	1790.9(2)	1430.5(1)	5592(1)	4673.2(2)
Z	4	2	3	8
μ(Mo Kα) (cm^{-1})	0.73	15.31	10.33	10.12
Reflection collected	8894	10033	2822	8205
Unique reflections	1826	8216	2248	6792
R_{int}	0.016	0.029	0.0325	0.0314
Residuals: *R* ($I > 2\sigma(I)$)	0.035	0.040	0.0339	0.0267
Residuals: *R*w ($I > 2\sigma(I)$)	0.101	0.100	0.0798	0.0539
Flack parameter	n.a.	−0.007(11)	−0.03(5)	−0.01(3)
Goodness-of-fit indicator	1.077	0.966	0.969	0.956

(8 mmol) was added to the mixture. A solution of alkyl diazoacetate (1 mmol) in CH_2Cl_2 (0.5 mL) was slowly added over 4 h. After the addition of ethyl diazoacetate, the mixture was allowed to stir for 16 h at room temperature. The mixture was worked-up as described above. For the cyclopropanation with *t*-butyl diazoacetate, enantiomeric excesses were determined by GC with a chiraldex *β*-PH column. For the competition reactions, styrene (2 mmol) and substituted styrene (2 mmol) were added to the catalytic solution generated from [Ru(**L**)(CO)Cl_2] (0.01 mmol) and AgOTf (0.02 mmol) in 0.63 mL CH_2Cl_2. Ethyl diazoacetate (0.5 mmol) was added in one portion to the reaction mixture. After 30 min, the reaction mixtures were checked with GC.

3. Results and discussion

3.1. Preparation of C_1-terpyridines *L1–3*

The synthesis of ligands **L1**–**3** is outlined in Scheme 1. Kröhnke condensations of 6-(1-pyridinioacetyl)-2,2′-bipyridine iodide with suitable α,*β*-unsaturated ketones in acetic acid at 120 °C for 12 h gave ligands **L1**–**3**. After washing with acetonitrile to dissolve colored impurities, the products were obtained as pale-yellow solid in 63%, 44% and 57% yields for **L1**, **L2** and **L3**, respectively. The ligands

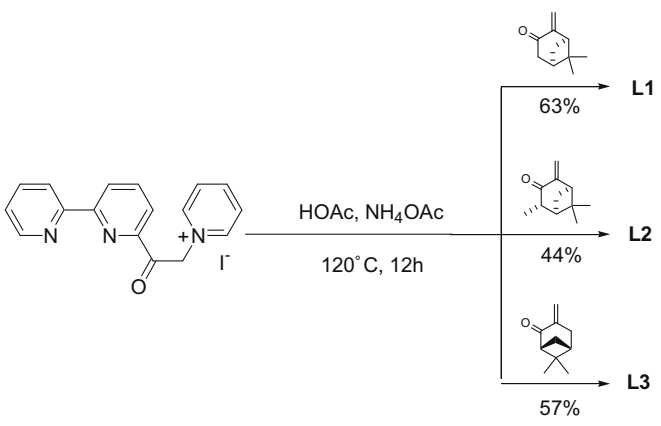

Scheme 1.

were characterized by ^{1}H NMR, ^{13}C NMR, IR and ESI-MS. From the ^{1}H NMR spectra of **L1**, **L2** and **L3**, nine sets of aromatic proton signals of the same integral ratio appeared as multiplets between 7.2 and 8.8 ppm. In addition, all ligands exhibited 15 sets of aromatic carbon signals from 117 to 161 ppm in their ^{13}C NMR spectra. For **L3**, crystals of X-ray quality were obtained by slow evaporation of a dichloromethane solution of **L3** and the structure is shown in Fig. 1. Similar to its C_2-counterpart [18], the pyridine rings adopt *transoid* configurations about the interannular C–C bonds. The three pyridine rings are not coplanar. Dihedral angle of the pyridine ring with the chiral moiety (12.2(2)°) is larger than the one without any substituent (6.1(3)°).

3.2. Complexes synthesis and characterization

The C_1-symmetric terpyridine copper(II) complexes [Cu(**L**)Cl_2] (**L1**–**3**) and rhodium(III) complexes [Rh(**L**)Cl_3] (**L1**–**3**) were prepared by methods that were similar to the synthesis for C_2-symmetric copper and rhodium complexes [10,12]. The copper complexes were isolated as green solids by reaction of a dichloromethane solution of the appropriate ligand with an ethanolic solution of $CuCl_2{\cdot}2H_2O$. The rhodium complexes were formed by treating the corresponding **L** with $RhCl_3{\cdot}3H_2O$ in refluxing ethanol. For all these C_1-symmetric copper and rhodium complexes, isolated yields were good and generally higher than their C_2-analog. Characterizations with elemental analysis showed that all the complexes exhibited a 1:1 metal to ligand ratio. For the ESI-MS analysis, fragmentation peaks corresponding to the loss of one Cl^- from the parent molecules were observed.

Crystals of [Cu(**L3**)Cl_2] suitable for X-ray structural analysis were grown by slow evaporation of a chloroform solution of [Cu(**L3**)Cl_2]. The molecular structure is shown in Fig. 2 while selected bond lengths and angles are listed in Table 2. The copper atom is surrounded by two chloride ions and three nitrogen atoms from a terpyridine. Coordination geometry around the copper atom can best be described as square pyramidal distorted trigonal bipyramid as the geometric parameters (τ) is observed to be 0.57 ($\tau = 0$ for ideal square pyramidal and $\tau = 1$ for ideal trigonal bipyramidal) [19]. This geometry is very different from that of the other achiral copper–terpyridine complexes, which are generally square pyramid as τ are in the range of 0.09–0.183 [20,21]. In the [Cu(**L3**)Cl_2], deviation from the ideal orthogonal arrangement between the

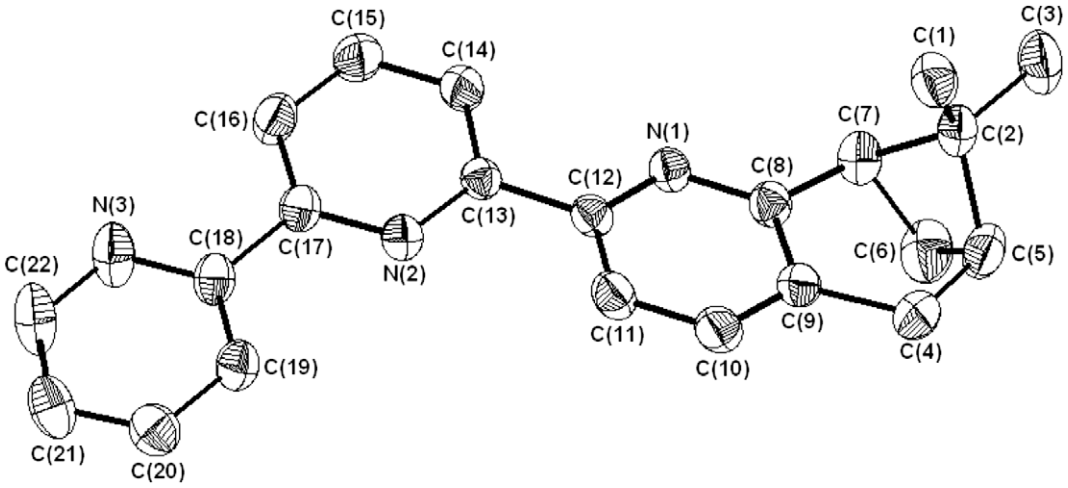

Fig. 1. Molecular structure of **L**3 including the atom numbering scheme. All hydrogen atoms have been omitted for clarity.

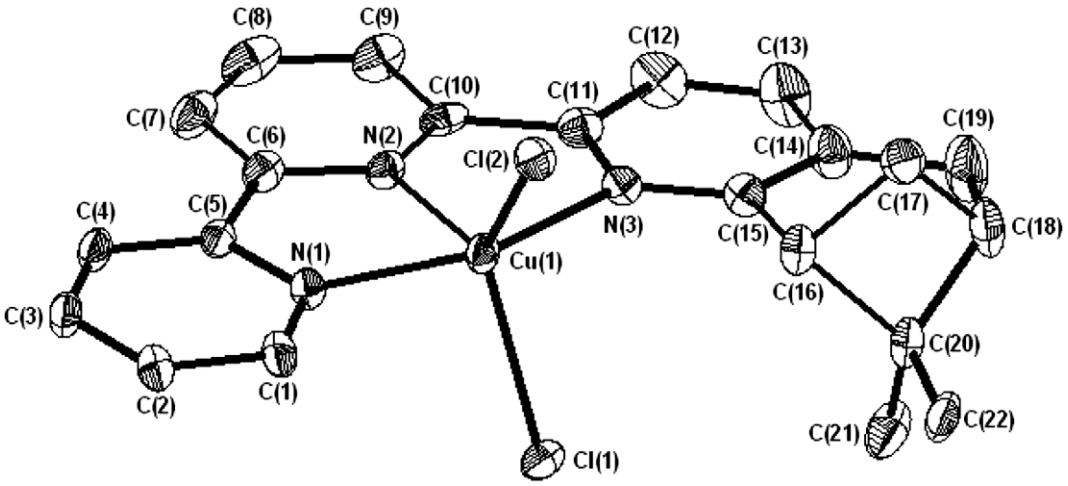

Fig. 2. ORTEP view for [Cu(**L3**)Cl_2] including the atom numbering scheme. All hydrogen atoms and solvent molecules have been omitted for clarity.

plane containing N(2)–Cl(1)–Cl(2) and the plane of the central pyridyl ring is less as the deviation angle is 3.87°. Indeed, the coordination geometry and the deviation angle in [Cu(**L3**)Cl_2] are similar to the corresponding C_2-symmetric complex, [Cu(**L6**)Cl_2] [18] in which τ and the deviation angle are 0.58 and 3.91°, respectively.

Table 2
Selected bond lengths (Å) and angles (deg) for [Cu(**L3**)Cl_2].

Bond lengths	
Cu(1)–Cl(1)	2.340(4)
Cu(1)–Cl(2)	2.311(3)
Cu(1)–N(1)	2.040(6)
Cu(1)–N(2)	1.972(5)
Cu(1)–N(3)	2.048(6)
Bond angles	
N(1)–Cu(1)–N(2)	78.3(2)
N(2)–Cu(1)–N(3)	79.7(2)
N(1)–Cu(1)–N(3)	158.0(2)
Cl(1)–Cu(1)–N(2)	123.6(1)
Cl(2)–Cu(1)–N(2)	123.0(2)
Cl(1)–Cu(1)–Cl(2)	113.14(5)
Cl(1)–Cu(1)–N(1)	94.9(1)
Cl(1)–Cu(1)–N(3)	96.7(1)
Cl(2)–Cu(1)–N(1)	93.0(1)
Cl(2)–Cu(1)–N(3)	99.6(1)

Nevertheless, the sterically less bulkiness of the C_1-symmetric complex can be reflected by the co-planarity of the terpyridine ligand. The average dihedral angle between the adjacent pyridyl rings in [Cu(**L3**)Cl_2] is 2.44° and this is smaller than the 9.38° in [Cu(**L6**)Cl_2]. Consequently, the bond distances between the copper and nitrogen atoms in [Cu(**L3**)Cl_2] (1.969(5), 2.035(7) and 2.050(6) Å) are shorter than those in [Cu(**L6**)Cl_2] (1.974(9), 2.075(4) and 2.080(3) Å).

Crystals of [Rh(**L1**)Cl_3] suitable for X-ray structural analysis were grown by slow evaporation of an ethanolic solution of [Rh(**L1**)Cl_3]. The crystal structure is shown in Fig. 3 and the selected bond distance and bond angles are given in Table 3. In the molecular structure, the six-coordinated rhodium atom is bound by three nitrogen atoms from **L1** and three chlorides to exhibit a distorted octahedral geometry. Similar to other Rh–terpyridine complex [12,22], the distortion is principally originated from the small bite angles of N(1)–Rh(1)–N(2) and N(2)–Rh(1)–N(3) (80.8(3) and 80.1(3)°, respectively), causing the N(1)–Rh(1)–N(3) angle of 160.6(3)° to deviate from the linearity. Moreover, the three pyridyl nitrogen–rhodium bond distances are not identical and the distances of Rh to the two distal nitrogens N(1) and N(3) (2.051(6) and 2.096(5) Å, respectively) are longer than the Rh–N(2) (1.940(9) Å).

In addition, bulky chiral moiety also exerts significantly to the geometric distortion. Steric interaction between an equatorial

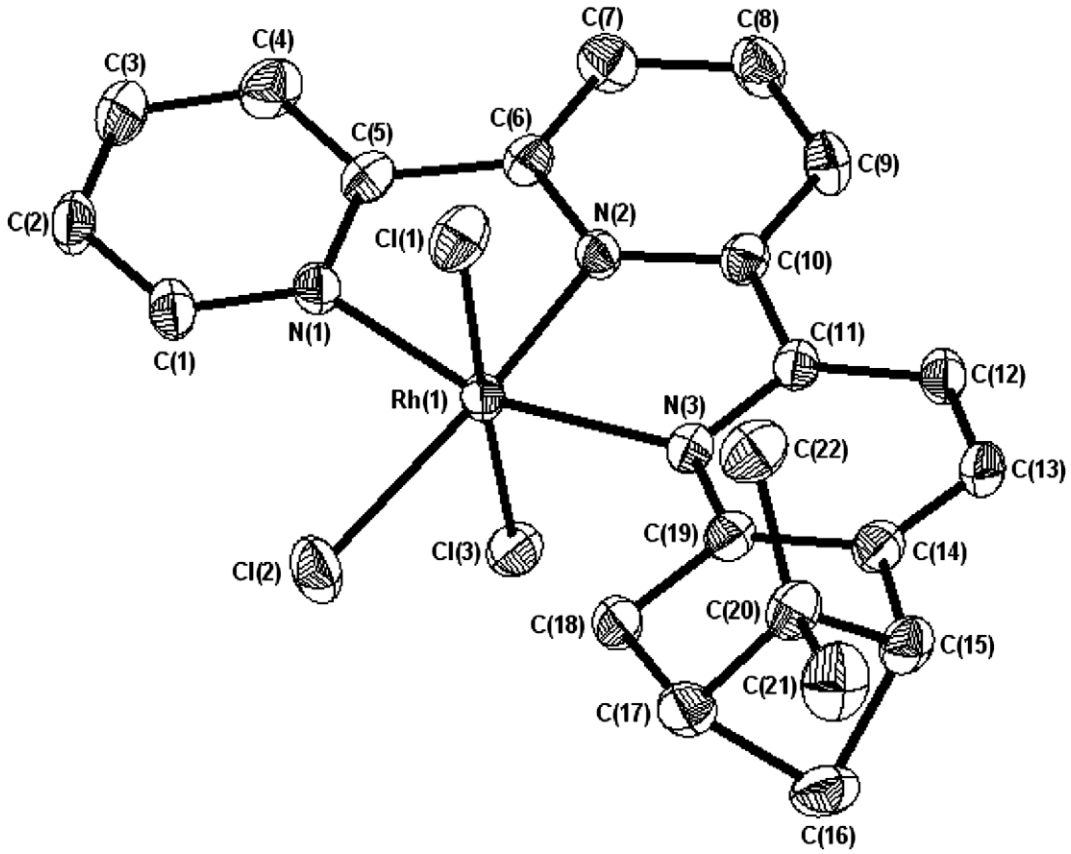

Fig. 3. ORTEP view for [Rh(**L1**)Cl_3] including the atom numbering scheme. All hydrogen atoms and solvent molecules have been omitted for clarity.

Table 3
Selected bond lengths (Å) and angles (deg) for [Rh(**L1**)Cl_3].

Bond lengths	
Rh(1)–Cl(1)	2.330(2)
Rh(1)–Cl(2)	2.375(3)
Rh(1)–Cl(3)	2.354(2)
Rh(1)–N(1)	2.051(6)
Rh(1)–N(2)	1.940(9)
Rh(1)–N(3)	2.096(5)
Bond angles	
C1(1)–Rh(1)–Cl(2)	93.07(8)
Cl(2)–Rh(1)–Cl(3)	89.72(8)
N(1)–Rh(1)–N(2)	80.8(3)
N(2)–Rh(1)–N(3)	80.1(3)
N(1)–Rh(1)–N(3)	160.6(3)
N(1)–Rh(1)–Cl(2)	92.3(2)
N(2)–Rh(1)–Cl(2)	171.0(2)
N(3)–Rh(1)–Cl(2)	107.1(2)
N(1)–Rh(1)–Cl(1)	89.7(2)
N(2)–Rh(1)–Cl(1)	90.9(2)
N(3)–Rh(1)–Cl(1)	87.3(2)
N(1)–Rh(1)–Cl(3)	90.3(2)
N(2)–Rh(1)–Cl(3)	86.4(2)
N(3)–Rh(1)–Cl(3)	91.8(2)

chloride atom Cl(2) and a carbon atom C(18) is partially relieved by displacing the Cl(2) away from the chiral moiety, as evidences by a larger angle of N(3)–Rh(1)–Cl(2) (107.1(2)°) than N(1)–Rh(1)–Cl(2) (92.3(2)°). However, for a corresponding C_2-symmetric complex, [Rh(**L4**)Cl_3] [11], the steric interaction is not simply relieved by the chloride displacement as the corresponding angles that are mentioned as above are similar to each other (99.9(2)° and 100.0(2)°). The steric interaction is relieved by twisting of the adjacent pyridyl rings (mean dihedral angle = 16.9°) and hence to result in a long bond distances between Rh and the N atoms from the two distal pyridyl units (2.111(5) and 2.110(5) Å). For the C_1-symmetric [Rh(**L1**)Cl_3], the mean dihedral angle is smaller 2.9° and the bond distances are shorter, Rh(1)–N(1) and Rh(1)–N(3) are 2.051(6) Å and 2.096(5) Å, respectively.

For the ruthenium complexes, [Ru(**L**)Cl_2] were firstly prepared by reacting 0.5 equiv of $[RuCl_2(p\text{-cymene})]_2$ to 1 equiv of **L** in refluxing ethanol/*n*-butanol. However, the products obtained gave complicated ^{1}H NMR spectra which may be attributed to the exchange of coordinated solvent molecules. This observation has been reported previously with a tridentate pyridyl-diimine ligand [23]. Therefore, no full characterizations of [Ru(**L**)Cl_2] have been made. Nevertheless, the stoichiometry of the complexes, [Ru(**L**)Cl_2], was revealed by coordinating with a DMSO molecule (Scheme 2). After addition of 1 equiv DMSO to [Ru(**L1**)Cl_2], the color of the reaction mixture changed immediately from violet to brown. After isolation and recrystallization of the product, ^{1}H NMR analysis showed that two compounds, in a ratio of 1:1, were presented. Unambiguous identification of the product was proceeded via X-ray structural analysis (*vide infra*). For the more bulky C_2-symmetric ligand **L4**, however, isolation of the DMSO complex resulted in failure. For ligands **L2** and **L3**, DMSO complexes were not prepared because existence of isomers as in the case of *cis*-[Ru(**L1**)(DMSO)Cl_2] precludes the development of selective catalyst.

Crystals of *cis*-[Ru(**L1**)(DMSO)Cl_2] suitable for X-ray structural analysis were grown by slow diffusion of distilled diethyl ether to an acetonitrile solution of *cis*-[Ru(**L1**)(DMSO)Cl_2]. As shown in Fig. 4, the structure revealed that two independent diastereomers A and B, differ in the position of the DMSO molecules relative to the dimethyl substituents (C(21) and C(22)) and (C(45) and C(46)) of chiral moieties on **L4**, are comprised in a unit cell. In these

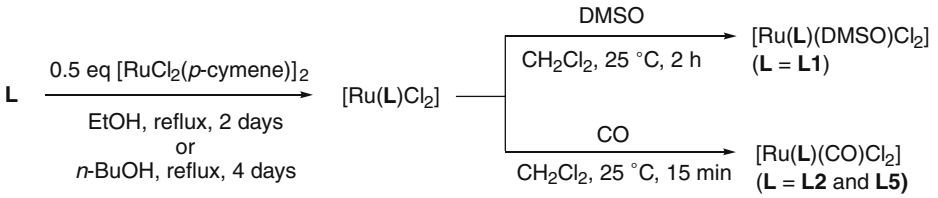

Scheme 2.

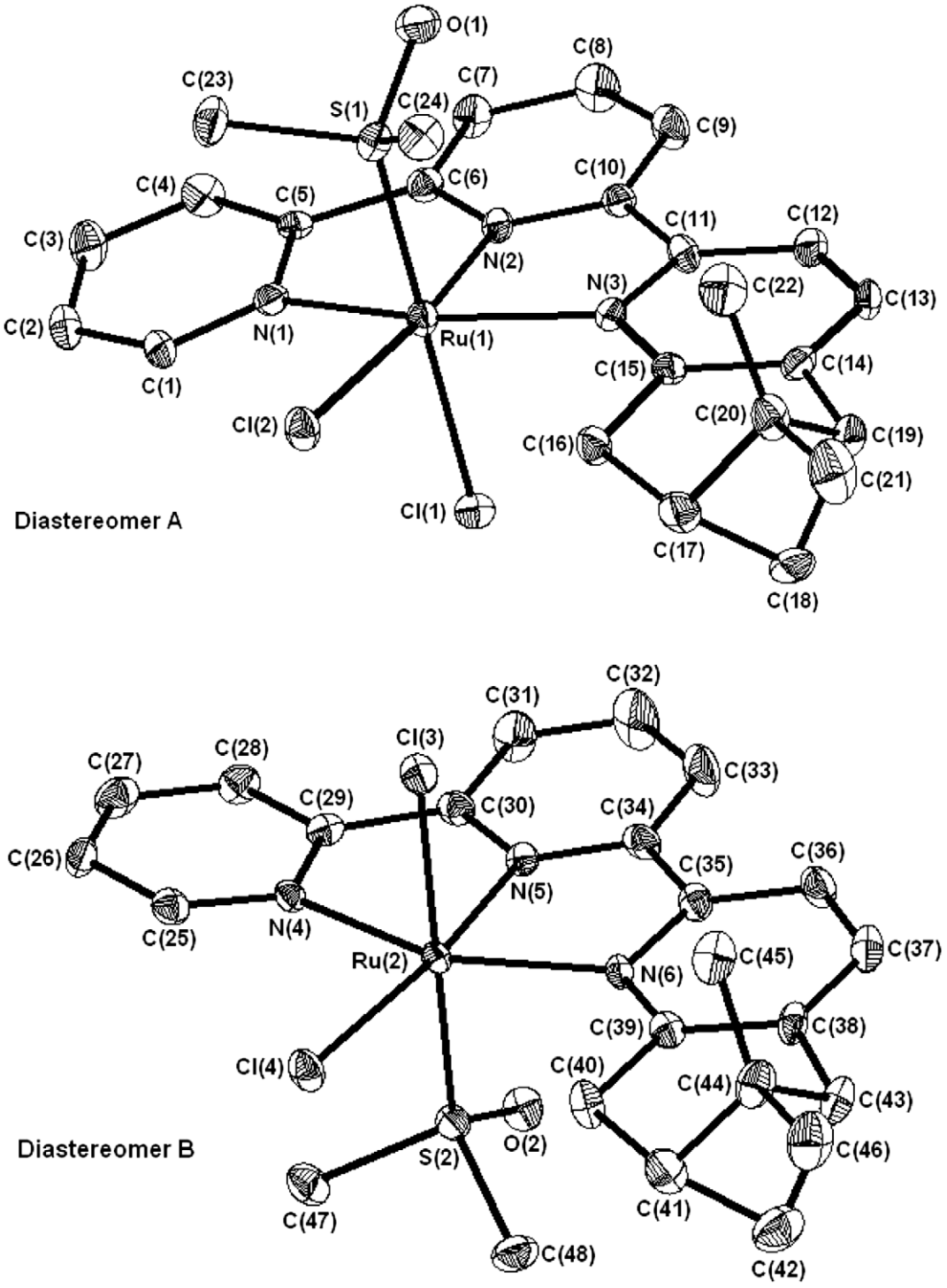

Fig. 4. ORTEP views for *cis*-[Ru(**L1**)(DMSO)Cl_2] including the atom numbering scheme. All hydrogen atoms and solvent molecules have been omitted for clarity (upper: diastereomer A, lower: diastereomer B).

Table 4
Selected bond lengths (Å) and angles (deg) for *cis*-[Ru(**L1**)(DMSO)Cl_2].

Diastereomer A		Diastereomer B	
Bond lengths		*Bond lengths*	
Ru(1)–N(1)	2.073(3)	Ru(2)–N(4)	2.072(3)
Ru(1)–N(2)	1.953(3)	Ru(2)–N(5)	1.961(3)
Ru(1)–N(3)	2.142(3)	Ru(2)–N(6)	2.140(3)
Ru(1)–Cl(1)	2.429(1)	Ru(2)–Cl(3)	2.418(1)
Ru(1)–Cl(2)	2.461(1)	Ru(2)–Cl(4)	2.455(1)
Ru(1)–S(1)	2.232(1)	Ru(2)–S(2)	2.222(1)
S(1)–O(1)	1.491(3)	S(2)–O(2)	1.475(3)
Bond angles		*Bond angles*	
C1(1)–Ru(1)–Cl(2)	91.99(4)	C1(3)–Ru(2)–Cl(4)	91.54(4)
Cl(1)–Ru(1)–S(1)	179.73(4)	Cl(3)–Ru(2)–S(2)	178.33(4)
S(1)–Ru(1)–Cl(2)	88.25(4)	S(2)–Ru(2)–Cl(4)	89.85(4)
N(1)–Ru(1)–N(2)	79.6(1)	N(4)–Ru(2)–N(5)	79.5(1)
N(2)–Ru(1)–N(3)	79.2(1)	N(5)–Ru(2)–N(6)	79.3(1)
N(1)–Ru(1)–N(3)	158.2(1)	N(4)–Ru(2)–N(6)	158.5(1)
N(2)–Ru(1)–Cl(1)	89.9(1)	N(5)–Ru(2)–Cl(3)	87.3(1)
N(1)–Ru(1)–Cl(1)	89.18(9)	N(4)–Ru(2)–Cl(3)	87.74(9)
N(3)–Ru(1)–Cl(1)	85.96(9)	N(6)–Ru(2)–Cl(3)	87.51(9)
N(1)–Ru(1)–S(1)	90.68(9)	N(4)–Ru(2)–S(2)	91.24(9)
N(2)–Ru(1)–S(1)	89.8(1)	N(5)–Ru(2)–S(2)	91.2 (1)
N(3)–Ru(1)–S(1)	94.07(9)	N(6)–Ru(2)–S(2)	92.97(9)
N(1)–Ru(1)–Cl(2)	93.47(9)	N(4)–Ru(2)–Cl(4)	93.71(9)
N(2)–Ru(1)–Cl(2)	172.2(1)	N(5)–Ru(2)–Cl(4)	173.1(1)
N(3)–Ru(1)–Cl(2)	107.95(9)	N(6)–Ru(2)–Cl(4)	107.42(9)
C(23)–S(1)–Ru(1)	113.2(2)	C(47)–S(2)–Ru(2)	112.6(2)
C(24)–S(1)–Ru(1)	113.7(1)	C(48)–S(2)–Ru(2)	115.3(1)
O(1)–S(1)–Ru(1)	117.1(1)	O(2)–S(2)–Ru(2)	116.4(1)
C(23)–S(1)–O(1)	105.1(2)	C(47)–S(2)–O(2)	106.6(2)
C(24)–S(1)–O(1)	107.3(2)	C(48)–S(2)–O(2)	105.7(2)
C(23)–S(1)–C(24)	98.6(2)	C(47)–S(2)–C(48)	98.6(2)

two structures, the coordination is similar. Coordination geometries for the Ru are octahedral, with a S-bonded DMSO molecule, two *cis* spanned Cl^- ions and three nitrogen atoms from **L4**. For their corresponding bond lengths and bond angles, no notable difference is observed as the deviations of them are not larger than 0.016 Å and 2.64°, respectively (Table 4). The bulky chiral moiety on **L4** exerts significant effect to the geometric distortion. As observed by the three asymmetric bond distances of the ruthenium-nitrogen bonds, the longest distances, Ru(1)–N(3) = 2.142(3) Å and Ru(2)–N(6) = 2.140(3) Å, are originated from the pyridyl rings with chiral moieties and these are significant longer than that from the side without chiral substituent (Ru(1)–N(1) = 2.073(3) Å and Ru(2)–N(4) = 2.072(3) Å). The shortest distance is from the middle pyridyl rings Ru(1)–N(2) = 1.953(3) Å and Ru(2)–N(5) = 1.961(3) Å. Moreover, steric interaction between the chiral moiety and equatorial chloride atoms Cl(2)/Cl(4) is observed to be more significant than that between the chiral moiety to the vertical molecules of bulky DMSO molecules. With diastereomer A as an example, the difference in angles of N(3)–Ru(1)–Cl(2) and N(1)–Ru(1)–Cl(2) is 14.48° which is larger than the difference in angles of 3.39° of N(3)–Ru(1)–S(1) and N(1)–Ru(1)–S(1). Similar observation has been found for diastereomer B as the two different angles are 13.71° and 0.23°, respectively.

Other than coordinating with the DMSO molecule, the stoichiometry of [Ru(**L**)Cl_2] can also be revealed by coordinating with a carbon monoxide molecule (Scheme 2). By bubbling CO into dichloromethane solutions of the [Ru(**L**)Cl_2] for 15 min, the complexes, *trans*-[Ru(**L**)(CO)Cl_2], could be isolated in good yields. The presence of CO in the complex was confirmed by the appearance of a strong absorption band at 1940–1950 cm^{-1} in the IR analyses [24] and a downfield chemical shift at 206.0–209.2 ppm in the ^{13}C NMR spectra [25]. For **L** = **L5**, the ^1H and ^{13}C NMR spectra suggested an overall C_2-symmetrical environment, implicating a *trans* arrangement of the two chloride ligands. For the C_1-symmetric **L2**, a *trans* arrangement is also proposed as only one isomer was observed with ^1H NMR. Carbonyl complexes with other C_1- and C_2-symmetric terpyridines are not reported because the catalytic re-

Table 5
Catalytic asymmetric cyclopropanation of styrene with diazoacetate with chiral copper(II), rhodium(III) and ruthenium(II) terpyridines.[a]

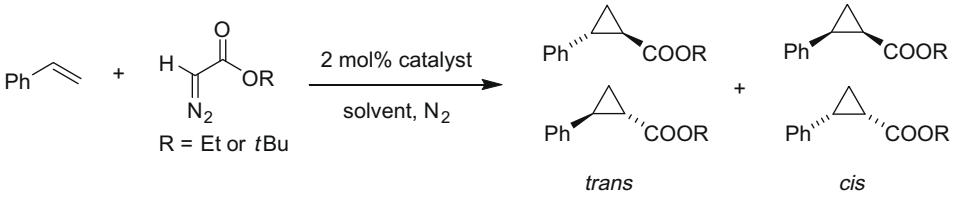

Entry	Complex	Yield (%)[b]	*Trans*/*cis*[c]	% ee[d]	
				trans	*cis*
1	[Cu(**L2**)Cl_2]	87	67:33	42(1*R*,2*R*)	60(1*R*,2*S*)
2[e]	[Cu(**L5**)Cl_2]	84	67:33	72(1*R*,2*R*)	82(1*R*,2*S*)
3	[Rh(**L2**)Cl_3]	29	42:58	7(1*R*,2*R*)	7(1*S*,2*R*)
4[e]	[Rh(**L5**)Cl_3]	54	30:70	65(1*S*,2*S*)	71(1*S*,2*R*)
5	[Ru(**L2**)(CO)Cl_2]	95	66:34	45(1*S*,2*S*)	26(1*S*,2*R*)
		98[f]	84:16	60(1*S*,2*S*)	67(1*S*,2*R*)
6	[Ru(**L5**)(CO)Cl_2]	93	48:52	19(1*S*,2*S*)	29(1*S*,2*R*)
		89[f]	52:48	55(1*S*,2*S*)	74(1*S*,2*R*)

[a] Copper, rhodium and ruthenium catalysts were generated by reactions of the complex with AgOTf and then with ethyl diazoacetate (EDA) (0.2 equiv). Reaction condition for [Cu(**L**)Cl_2]: AgOTf (2 equiv), catalyst/EDA/styrene = 1:50:200, CH_2Cl_2, 25 °C, 4 h addition of EDA and then stirring for 16 h. For [Rh(**L**)Cl_3]: AgOTf (4 equiv), catalyst/EDA/styrene = 1:50:250, THF, 25 °C, 4 h addition of EDA and then stirring for 16 h. For [Ru(**L**)(CO)Cl_2]: AgOTf (2 equiv), catalyst/EDA/styrene = 1:50:400, CH_2Cl_2, 25 °C, 4 h addition of EDA and then stirring for 16 h.

[b] Isolated yields of cyclopropanes are based on expected product.

[c] Determined by GC-FID.

[d] Enantiomeric excesses were determined with chiral columns on a HPLC or GC-FID. Absolute configurations were determined by comparing the order of elution of samples with known configuration.

[e] Data were obtained from reference [13].

[f] *t*-Butyl diazoacetate was employed instead of EDA.

sults are not as good as **L2** and **L5** in the preliminary screening for cyclopropanation.

3.3. Catalytic cyclopropanation reactions

For the copper and rhodium catalyzed cyclopropanation, the reaction conditions that were employed are the same as the previously study for C_2-symmetric copper and rhodium complexes [13]. For the ruthenium catalyzed cyclopropanation, active catalysts were generated by reacting the [Ru(**L**)(CO)Cl_2] with 2 equiv of AgOTf. After some optimization of conditions, a ratio of catalyst/alkyl diazoacetate/styrene of 1:50:400 which give fair to good yields of cyclopropanes as major products were employed. All of the copper, rhodium and ruthenium catalysts are active catalysts for cyclopropanation of styrene with ethyl diazoacetate (EDA) or *t*-butyl diazoacetate (TDA). Because the **L2** and **L5** gave the highest% ee and hence can be lead to a more meaningful discussion in reactive intermediate, only the results with these two ligands are discussed further. The catalytic activities of these complexes are shown in Table 5.

The effects of C_1- and C_2-symmetry on the catalytic cyclopropanation depend very much on the metal systems. In general, for the copper (entries 1 versus 2) and ruthenium (entries 5 versus 6) systems, the yields of cyclopropane from cyclopropanation of styrene with EDA or TDA from the C_1-symmetric catalysts are higher than that from the C_2-catalysts. But this is not the case for the rhodium system. C_1-Symmetric [Rh(**L2**)Cl_3] gave a significantly lower yield of cyclopropane than the C_2-catalyst (entries 3 versus 4). Moreover, ratios of *trans*/*cis* of the cyclopropanes of styrene with EDA from the rhodium and ruthenium systems are affected notably with the symmetry of the ligands. Both systems from the C_1-symmetric ligand **L2** result in higher *trans*-cyclopropanes selections than the corresponding C_2-catalysts as the *trans*/*cis* ratios of C_1 versus C_2 are 42:58 versus 30:70 for the rhodium and 66:34 versus 48:52 for the ruthenium. In particular to the ruthenium catalysts, when a more bulky TDA were employed, the *trans*/*cis* ratio from the C_1-catalyst increased significantly to 84:16 but it increased only slightly to 52:48 for the C_2-system. For the copper catalysts, the *trans*/*cis* ratios (67:33) for the C_1- and C_2-systems are equal. Furthermore, enantioselectivities were also varied in different extent with ligand symmetry from the different metal systems. For the ruthenium catalysts, no matter whether with EDA or TDA, C_1-catalyst always results in higher% ee for the *trans*-isomers (45% and 60%) than the C_2-catalyst (19% and 55%). C_1-catalyst give slightly lower% ee for the *cis*-isomers (26% and 67%) than the C_2-catalyst (29% and 74%). For the copper and rhodium systems, C_1-catalysts resulted in lower% ee of both the *trans* and *cis* cyclopropanes when compared with the corresponding C_2-systems (entries 1 versus 2 and 3 versus 4). Apart from the enantioselectivity, absolute configurations of the cyclopropanes are varied with the ligand symmetry in some cases. For the rhodium, the *trans* cyclopropane from the C_1-system is in opposite absolute configuration to the C_2-catalyst. But the reverse in configuration is not observed for the *cis*-cyclopropane (entries 3 versus 4). For the copper and ruthenium, the absolute configurations of cyclopropanes from the C_1- and C_2-catalysts remained the same in each case.

To get more information about the effects of C_1- and C_2-symmetry on the nature of the intermediates involved, the rates of cyclopropanation of substituted styrenes relative to styrene with EDA were measured through competition experiments using *trans*-[Ru(**L**)(CO)Cl_2] (**L2** and **L5**), [Cu(**L2**)Cl_2] and [Rh(**L2**)Cl_3]. The Hammett plots of $\log(k_X/k_H)$ versus σ^+ for these catalysts are shown in Figs. 5–8. The results of the previously reported competitions

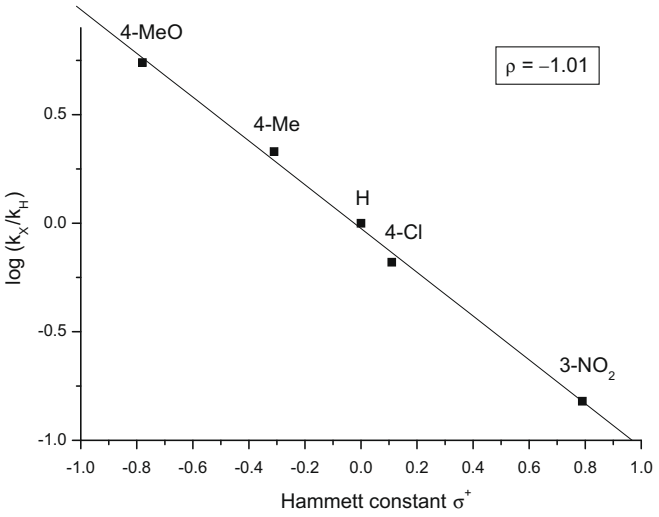

Fig. 6. Hammett plot for the cyclopropanation of styrene with EDA using *trans*-[Ru(L5)(CO)Cl_2] as catalyst precursor.

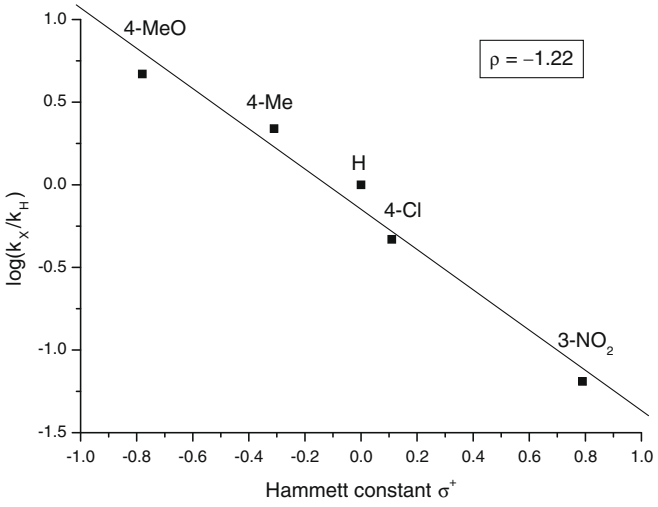

Fig. 5. Hammett plot for the cyclopropanation of styrene with EDA using *trans*-[Ru(**L2**)(CO)Cl_2] as catalyst precursor.

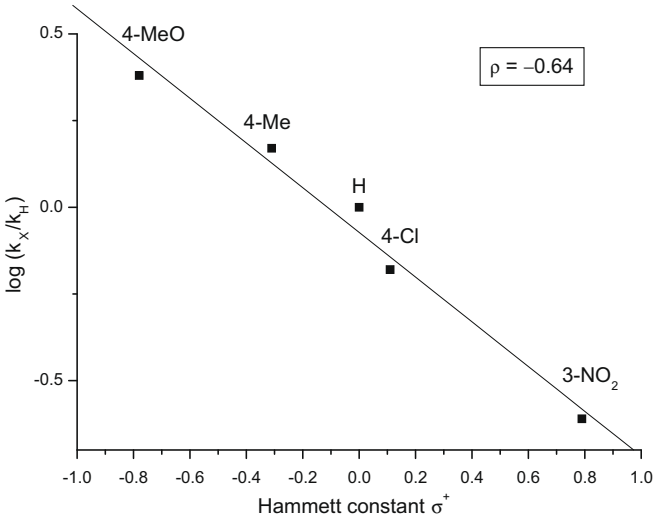

Fig. 7. Hammett plot for the cyclopropanation of styrene with EDA using [Cu(L2)Cl_2] as catalyst precursor.

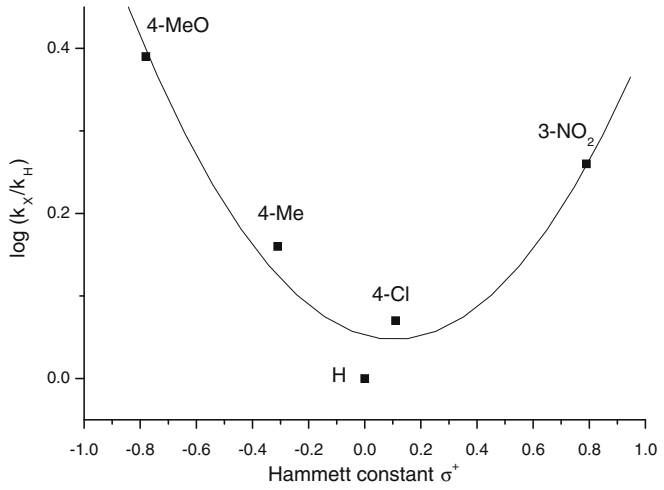

Fig. 8. Hammett plot for the cyclopropanation of styrene with EDA using [Rh(L2)Cl_3] as catalyst precursor.

with C_2-symmetric [Cu(**L5**)Cl_2] and [Rh(**L5**)Cl_3] are used for comparison [13]. For both of the C_1- and C_2-ruthenium systems, the electron-donating substituted styrenes increased the reaction rates while their electron-withdrawing counterparts produced a decrease. Both of them followed linear σ^+ correlation (R^2 = 0.97–0.99) with a slightly larger (more negative) value of ρ for C_1-catalyst (−1.22) than that for C_2-catalyst (−1.01). Nevertheless, these values are smaller than the ruthenium–PNNP catalyst (ρ = −2.40 correlating to σ_{para}) [26] but significantly larger than the ruthenium–porphyrin system (ρ = 0.44 correlating to σ^+) [27]. Correlation to the σ^+ in these ruthenium–terpyridine systems imply that the intermediates are much more closely resembles the porphyrin system (which has been proposed to have a built-up positive charge in the intermediate) than the PNNP system. The larger ρ values indicate that the intermediate for the ruthenium–terpyridine catalyst are more electrophilic than that for the ruthenium–porphyrin catalyst. For the copper systems, similar to ruthenium systems, both of the C_1- and C_2-catalysts gave linear σ^+ correlation (R^2 = 0.98–0.99). However, the ρ from C_1-copper (−0.64) is smaller (less negative) than that for the C_2-copper (−0.76) [13]. And the ρ for both C_1- and C_2-catalysts lied within the range of ρ for other copper catalysts with ligands such as tris(pyrazolyl) borate (ρ = −0.85 correlating to σ) [28] and bisoxazoline (ρ = −0.51 correlating to σ^+) [29]. The best fit correlations of the data points to σ^+ reveal that the copper–terpyridine systems resemble to the copper–bisoxazoline system and the intermediate are more electrophilic than the copper–bisoxazoline system as a larger ρ is observed in the copper–terpyridine systems. For the rhodium systems, the Hammett plot of C_1-symmetric catalyst showed a non-linear U-shaped relationship with σ^+. And this observation is very different from the negative linear correlation with σ^+ for the C_2-catalyst [13]. Hence this may reveal the drastic difference in catalytic reactivity for the C_1- and C_2-catalysts (Table 5, entries 3 and 4). The non-linearity might suggest the presence of active intermediates that have significant radical character [30] or two pathways of similar activation energies [31] in the reaction. A study of non-linear correlations in catalytic cyclopropanation with iron- and cobalt-terpyridine systems has been reported by our group recently [32].

Based on the absolute configurations of the products obtained from the catalytic cyclopropanation with C_1- and C_2-symmetric copper, ruthenium and rhodium catalysts (Table 5), some information that related to the mechanism can be obtained. For the copper systems, the absolute configurations of the *trans*-cyclopropanes (1*R*,2*R*) or *cis*-cyclopropanes (1*R*,2*S*) from the C_1- and C_2-catalysts are the same. This observation suggests that a similar model, with a horizontal carbene, which was proposed previously [33] can be applied in the case of C_1-catalyst. For the C_1-rhodium system, the asymmetric induction for the *trans*- and *cis*-cyclopropanes are reversed. This observation suggests that different intermediate might involve with C_1- and C_2-rhodium catalyst [13]. For the ruthenium systems, both C_1- and C_2-catalysts gave the same absolute configurations of (1*S*,2*S*) and (1*S*,2*R*) for the *trans*- and *cis*-cyclopropanes, respectively, which are the same as the C_2-rhodium catalyst. A model that is similar to C_2-rhodium catalyst [13] is proposed here. However, the exact nature of the intermediate is under investigation.

4. Conclusion

In summary, chiral terpyridine ligands of copper(II) complexes, of formula [Cu(**L**)Cl_2], rhodium(III) complexes, of formula [Rh(**L**)Cl_3] and ruthenium(II) complexes, of formula *cis*- or *trans*-[Ru(**L**)(X)Cl_2] (X = DMSO or CO), are effective catalysts that afford cyclopropyl esters in good yield. Moderate enantioselectivities of up to 74% ee have been obtained with complexes having chiral C_1 and C_2-terpyridines. We are continuing our effort to metal-terpyridine catalysts for other reactions.

5. Supplementary data

CCDC 703308, 736281, 736282, and 736283 contain the supplementary crystallographic data for **L3**, [Cu(**L3**)Cl_2], [Rh(**L1**)Cl_3] and [Ru(**L1**)(DMSO)Cl_2] respectively. These data can be obtained free of charge via http://www.ccdc.cam.ac.uk/conts/retrieving.html, or from the Cambridge Crystallographic Data Center, 12 Union Road, Cambridge CB2 1EZ, UK; fax: (+44) 1223-336-033; or e-mail: deposit@ccdc.cam.ac.uk.

Acknowledgements

Financial support for this research from the Hong Kong Research Grants Council the Area of Excellence Scheme established under the University Grants Committee of the Hong Kong SAR, China (Project No. AoE/P-10/01) and GRF grant (CityU 101108). are gratefully acknowledged.

References

[1] K.M.-C. Wong, V.W.-W. Yam, Coord. Chem. Rev. 251 (2007) 24772488.
[2] S. Bonnet, J.-P. Collin, J.-P. Sauvage, Inorg. Chem. 46 (2007) 1052010533.
[3] F. Liu, T. Cardolaccia, B.J. Hornstein, J.R. Schoonover, T.J. Meyer, J. Am. Chem. Soc. 129 (2007) 24462447.
[4] C. Duboc, M.-N. Collomb, J. Pécaut, A. Deronzier, F. Neese, Chem. Eur. J. 14 (2008) 64986509.
[5] B. Hasenknopf, J.-M. Lehn, G. Baum, D. Fenske, Proc. Natl. Acad. Sci. USA 93 (1996) 13971400.
[6] U.S. Schubert, H. Hofmeier, G.R. Newkome, Modern Terpyridine Chemistry, Wiley-VCH, Weinheim, 2006.
[7] E.C. Constable, Chem. Soc. Rev. 36 (2007) 246253.
[8] R. Ziessel, Synthesis 1999 (1999) 18391865.
[9] C.-T. Yeung, H.-L. Yeung, C.-S. Tsang, W.-Y. Wong, H.-L. Kwong, Chem. Commun. (2007) 52035205.
[10] G. Chelucci, A. Saba, D. Vignola, C. Solinas, Tetrahedron 57 (2001) 10991104.
[11] M. Ziegler, V. Monney, H. Stoeckli-Evans, A. Von Zelewsky, I. Sasaki, G. Dupic, J.-C. Daran, G.G.A. Balavoine, J. Chem. Soc., Dalton Trans. (1999) 667. 676.
[12] H.-L. Kwong, W.-S. Lee, Tetrahedron: Asymmetry 11 (2000) 22992308.
[13] H.-L. Kwong, W.-L. Wong, W.-S. Lee, L.-S. Cheng, W.-T. Wong, Tetrahedron: Asymmetry 12 (2001) 26832694.
[14] M.P. Hartshorn, A.F.A. Wallis, J. Chem. Soc. (1964) 52545260.
[15] C. Bolm, M. Ewald, M. Felder, G. Schlingloff, Chem. Ber. 125 (1992) 11691190.
[16] E.C. Constable, G. Baum, E. Bill, R. Dyson, R. Van Eldik, D. Fenske, S. Kaderli, D. Morris, A. Neubrand, M. Neuburger, D.R. Smith, K. Wieghardt, M. Zehnder, A.D. Zuberbühler, Chem. Eur. J. 5 (1999) 498508.
[17] F. Kröhnke, Synthesis (1976) 124.

[18] F. Pezet, I. Sasaki, J.-C. Daran, J. Hydrio, H. A-Haddou, G. Balavoine, Eur. J. Inorg. Chem. (2001) 26692674.
[19] A.W. Addison, T.N. Rao, J. Reedijk, J. van Rijn, G.C. Verschoor, J. Chem. Soc., Dalton Trans. (1984) 1349. 1356.
[20] W. Henke, S. Kremer, D. Reinen, Inorg. Chem. 22 (1983) 28582863.
[21] T. Rojo, M. Vlasse, D. Beltran-Porter, Acta Crystallogr., Sect. C39 (1983) 194199.
[22] F.P. Pruchnik, P. Jakimowicz, Z. Ciunik, J. Zakrzewska-Czerwińska, A. Opolski, J. Wietrzyk, E. Wojdat, Inorg. Chim. Acta 334 (2005) 5966.
[23] B. Cetinkaya, E. Cetinkaya, M. Brookhart, P.S. White, J. Mol. Catal. A 142 (1999) 101. 112.
[24] G.B. Deacon, J.M. Patrick, B.W. Skelton, N.C. Thomas, A.H. White, Aust. J. Chem. 37 (1984) 929945.
[25] H. Nishiyama, Y. Itoh, Y. Sugawara, H. Matsumoto, K. Aoki, K. Itoh, Bull. Soc. Jpn. 68 (1995) 12471262.
[26] S. Bachmann, A. Mezzetti, Helv. Chim. Acta 84 (2001) 30633074.
[27] C.-M. Che, J.-S. Huang, F.-W. Lee, Y. Li, T.-S. Lai, H.-L. Kwong, P.-F. Teng, W.-S. Lee, W.-C. Lo, S.-M. Peng, Z.-Y. Zhou, J. Am. Chem. Soc. 123 (2001) 41194129.
[28] M.M. Diaz-Requejo, P.J. Pérez, M. Brookhart, J.L. Templeton, Organometallics 16 (1997) 43994402.
[29] T. Rasmussen, J.F. Jensen, N. Østergaard, D. Tanner, T. Ziegler, P.-O. Norrby, Chem. Eur. J. 8 (2002) 177184.
[30] D.W. Nelson, A. Gypser, P.T. Ho, H.C. Kolb, T. Kondo, H.-L. Kwong, D.V. McGrath, A.E. Rubin, P.-O. Norrby, K.P. Gable, K.B. Sharpless, J. Am. Chem. Soc. 119 (1997) 18401858.
[31] N.S. Isaacs, Physical Organic Chemistry, Longman Scientific and Technical, Harlow, 1987.
[32] C.-T. Yeung, K.-C. Sham, W.-S. Lee, W.-T. Wong, W.-Y. Wong, H.-L. Kwong, Inorg. Chim. Acta 362 (2009) 32673273.
[33] W.-L. Wong, W.-S. Lee, H.-L. Kwong, Tetrahedron: Asymmetry 13 (2002) 14851492.